MULTISENSOR RECEIVER FOR MOBILE COMMUNICATIONS: AN EXPERIMENTAL STUDY

J.F DIOURIS[1], J. SAILLARD[1], A.C. TAROT[2], C. TERRET[2], J.P. BLOT[3]

[1]Laboratory Systèmes Electronique et Informatiques
IRESTE, Nantes, France
[2]Laboratory Antennes et Microélectronique
University of Rennes, Rennes, France
[3]Centre National d'Etudes des Télécommunications
PaB/STS/ANT, La Turbie, France

ABSTRACT

This paper presents the experimental study of a multisensor receiver for mobile communications. A five sensors receiver is described. Its aim is the measurement of received signals on several sensors for characterization and test of diversity algorithms. Measurements were made with different antennas arrays, locations and data rates. Results are obtained for a data rate equal to 200 kbit/s. The signal to noise ratio obtained on the sensors is evaluated and compared. An implementation of a blind adaptive algorithm is proposed and finally, its performance is examined on the measured data.

1. INTRODUCTION

New possibilities in the miniaturization of high frequency receivers allow to consider the use of several sensors in radiomobile receivers. In the case of flat fading i.e when the bandwidth of the signal is smaller than the inverse of the channel delays spread, a simple combination scheme can be used. Diversity is effective because the probability of simultaneously having a low signal to noise ratio on each sensors is small.

The paper is organized as follows:

Firstly the multisensor receiver, built in order to record signals in the same manner as a real-time receiver, is described.

Then the measurements are presented: the receiver was placed on a vehicle and signals were recorded in different locations, with several data rates and antennas arrays.

A diversity algorithm is chosen and implemented. Then the signal to noise ratio obtained on each sensor after demodulation is studied and compared.

Finally the performance of the diversity algorithm is studied on the measured data.

2. EXPERIMENTAL RECEIVER

The receiver owns five sensors. The considered algorithms need coherent measurements of the sensors signals. They are digitized after frequency converters which use a common local oscillator.

The receiver sensitivity is -90 dBm. The carrier frequency is 1491 MHz. An automatic gain control maintains the signals level in the dynamic of the analog to digital converters (ADC).

The digitized signals are filtered by transverse filters in order to obtain phase and quadrature projection. After this process, the sampling frequency can be fixed between 100 Hz and 1 MHz.

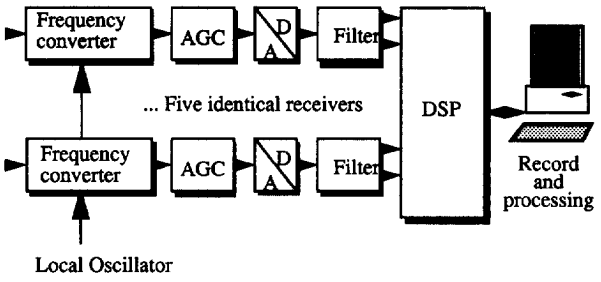

figure 1 : Experimental receiver

3. MEASUREMENTS

The measurements were done during July 1994 in the south of France (La Turbie). Several types of measurements were carried out with different antennas arrays, locations of measurements and data rates. But only one type of records is studied in the second part of this paper.

3.1. Antennas arrays

From the different types of array used during the measurements, two are of particular interest (figure 2):

. a planar circular array of five patch antennas
. a pyramidal array using the same antennas

3.2. Location of the measurements

The transmitter was placed on a 500 meters high hill overhanging the principality of Monaco. As indicated on the map in figure 3, the vehicle was moving in a suburban and urban area. Due to the altitude of the transmitter, there was sometimes a direct link. But downtown, the received signal is essentially due to multipath without visibility. In this situation the signal modulus is Rayleigh distributed

The transmitter power was 40 W. The average received levels were measured and are plotted on the

1058-6393/95 $4.00 © 1995 IEEE

map. It varies between -100 and -65 dBm. The largest value corresponds to the case of visibility. The lowest is obtained when the distance between transmitter and receiver is the largest. In lot of cases the obtained value is close to the sensibility of the receiver.

3.3. Data rate and sampling frequency

Measurements were made for several data rates from 8 kbit/s to 1 Mbit/s. In this paper we are interested by the data rate of 200 kbit/s. This value is under GSM data rate (270 kbit/s). The symbol duration in the case of a QPSK modulation is 10 µs. Most of the time, the channel can be considered as a non-selective channel.

A sampling frequency of 1 MHz was used, giving ten samples by symbol.

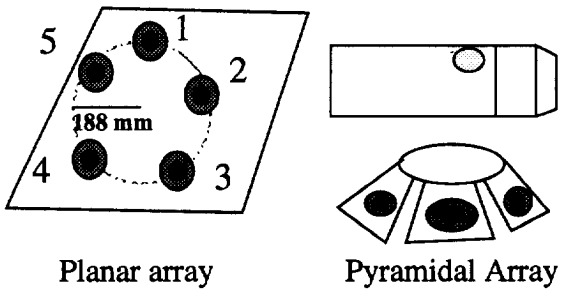

figure 2 : Antennas arrays

4. ALGORITHM

4.1. RLS Algorithm

The sensor signals are weighted and summed by means of classical spatial filter defined by:

$$y(t) = W^t X(t) \tag{1}$$

where y(t) is the array output, W is the weights vector and X(t) is the input signal vector.

The objective of the algorithm is to minimize the error power between the array output and a reference signal d(t). This error is defined by:

$$\zeta(W) = \sum_{i=1}^{K} \alpha^{K-i} |y(i) - d(i)|^2 \tag{2}$$

A simple algorithm can be [1] :

$$\begin{aligned} M_{k+1} &= X^*(k+1)X^t(k+1) + \alpha M_k \\ r_{k+1} &= X^*(k+1)d(k+1) + \alpha r_k \\ W_{k+1} &= M_{k+1}^{-1} r_{k+1} \end{aligned} \tag{3}$$

Where M is the weighted time-average covariance matrix, r is the weighted time-average cross-correlation vector between the signal vector and the reference signal and α is the weighting factor.

4.2. Implementation

For the implementation of this algorithm, the following points must be examined.

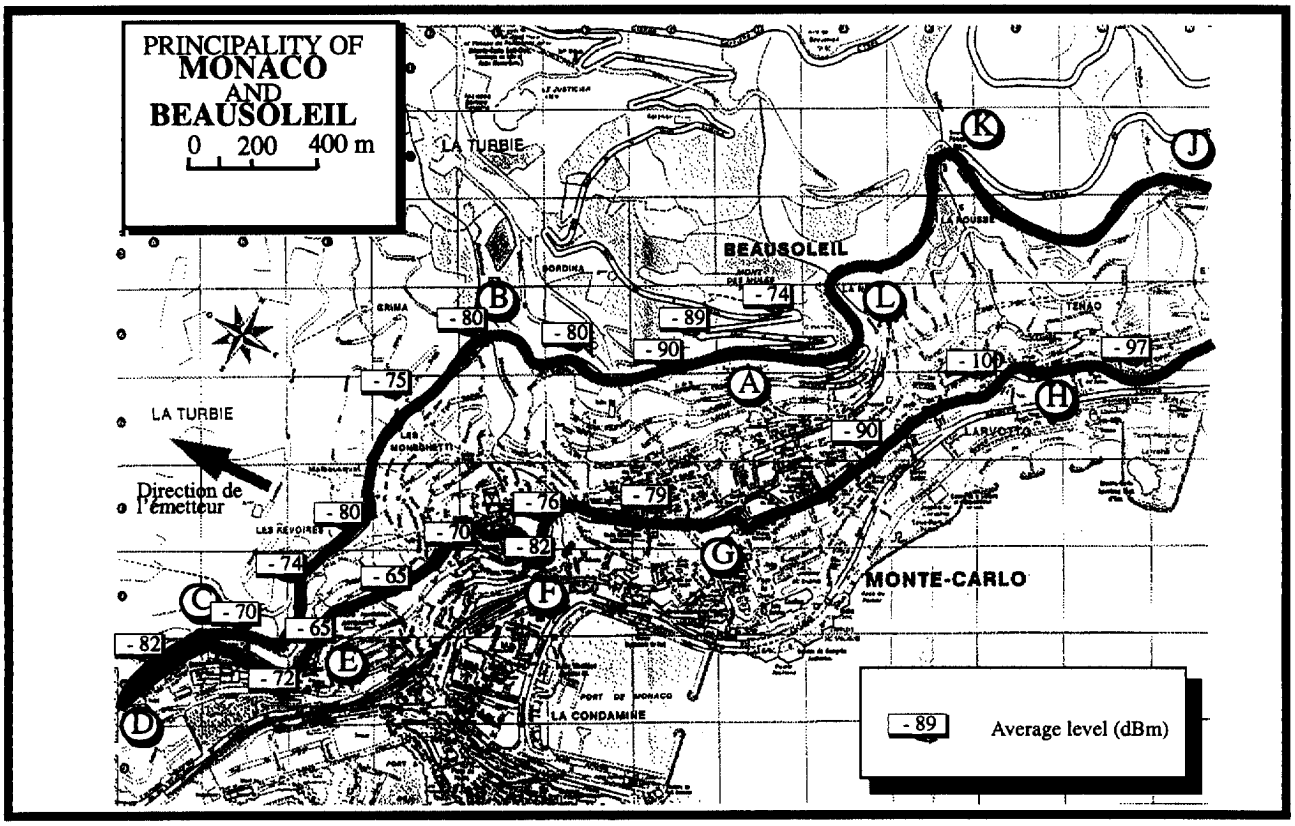

4.2.1. Reference signal generator

Two solutions are available to build the reference signal.

a) A learning sequence is transmitted. This solution is expensive in data rate but the convergence is guaranteed.

b) Blind adaptation. This solution is only possible if the error rate is not high at the beginning of the algorithm.

The last solution is chosen here, because of its simplicity.

4.2.2. Synchronization with the symbol timing

The algorithm works once per symbol. It must be synchronized with the symbol timing.

4.2.3. QPSK demodulator

A coherent demodulator is used (figure 3) with an early-late synchronizer for the symbol timing and a Costas loop for the carrier phase recovery.

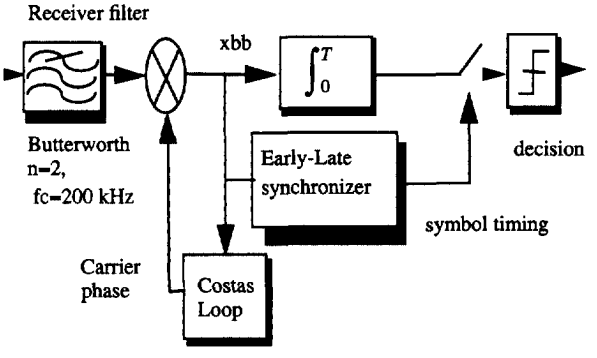

figure 3 : QPSK demodulator

4.2.4. Propagation delays in the operators

The block-diagram of the receiver is given in figure 4. The propagation delays of the different blocks are zero except for the QPSK demodulator. In this device, the decision is made at the end of the symbol and is validated during the following symbol. This is illustrated in figure 5.

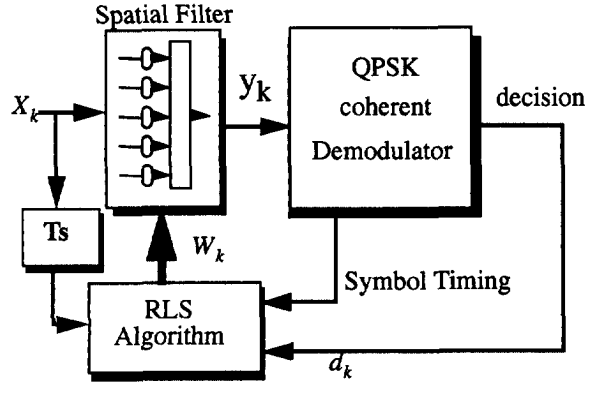

figure 4 : Block diagram of the adaptive receiver

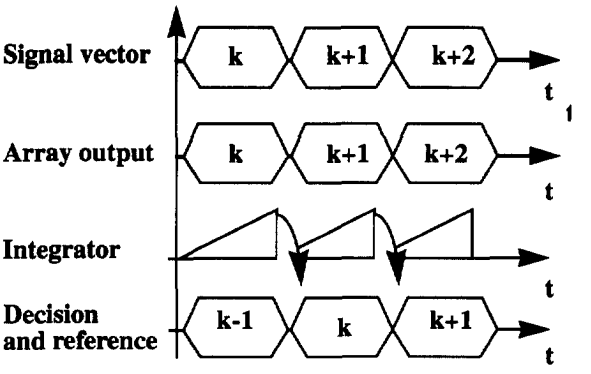

figure 5 : Propagation delays in the demodulator

Consequently, it is necessary to introduce a symbol delay in the signal vector paths.

4.3. Theoretical performance for a simple signals scenario

First we consider a flat fading scenario. The useful signal is arriving on each sensor with different signal to noise ratios. The intersymbol interference due to multipath is negligeable. The signal obtained on each sensor k is given by:

$$x_k(t) = \alpha_k s(t) + n_k(t) \tag{4}$$

where α_k is a complex number, s(t) is the unity power useful signal and $n_k(t)$ is the noise.

It is well known that, in this case, the obtained weights are [1]:

$$w_k = \mu \frac{\alpha_k^*}{\sigma_k^2} \tag{5}$$

where μ is a constant, σ_k are the noise power on each sensor. The instantaneous signal to noise ratio at the output of the array is the sum of the instantaneous signal to noise ratios on each sensor:

$$\gamma = \sum_{k=1}^{K} \frac{|\alpha_k|^2}{\sigma_k^2} = \sum_{k=1}^{K} \gamma_k \tag{6}$$

5. Diversity

First the five obtained signals are demodulated by identical but independent demodulators. The signal to noise ratio (SNR) is then computed in the middle of each symbol, after phase recovery. Figure 6 shows an example of the signals obtained on the five sensors after carrier recovery. The SNR are quite different on the five sensors.

Figure 7 gives the correlation between SNR estimated on each sensor. These results are obtained after the processing of 50 records. This plot exhibits a very low correlation between the sensors.

These results are given for a planar array. Results for the pyramidal array are essentially identical except in visibility with low incidence. In this case, one of the sensor

presents regularly the highest SNR.

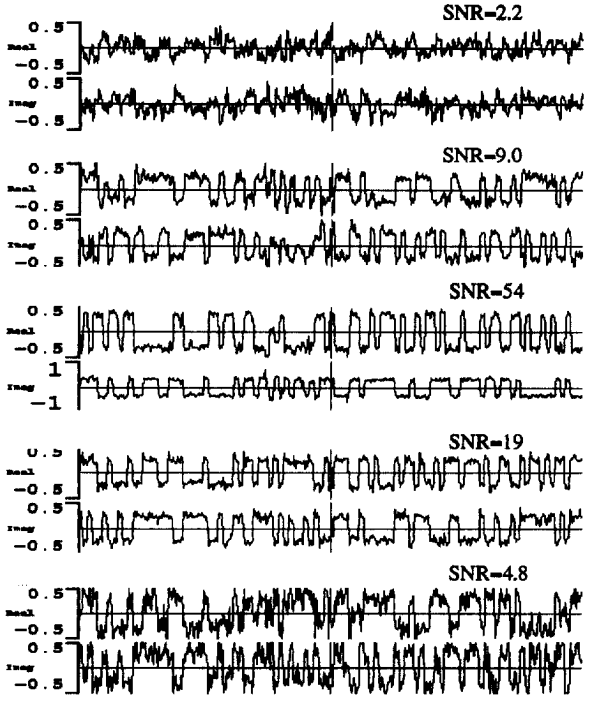

figure 6 : Signals on the five sensors after carrier recovery (1000 samples, 1 ms)

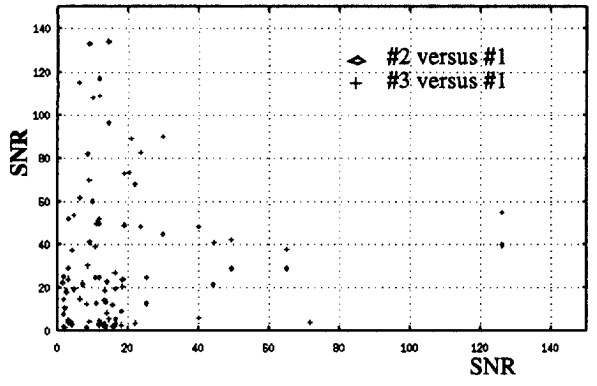

figure 7 : Correlation of SNR on the different sensors

6. Algorithm results

In this section, the results of the application of the proposed algorithm to the measured data is discussed. First an example is detailed. Secondly, statistical results are given from trials on 50 records. Finally, some explanations are given on the results obtained.

6.1. A detailed example

Figures 8 to 11 show a detailed study. This example was recorded near point D (see the map). There was no visibility. The planar array was used.

Figure 8 shows 2000 samples (i.e. 2 ms) of the signals measured on each sensors. In comparing the SNR given in figure 8 and the weights plotted in figure 9, it can be noticed that the sensors with the larger SNR are selected (i.e. number 2, 3 and 5). The output SNR is 93 which is three times the mean SNR on the sensors.

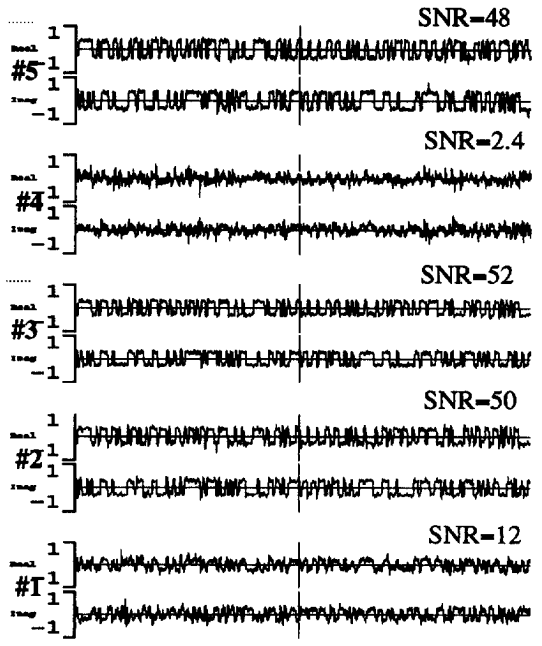

figure 8 : Signals on the five sensors after carrier recovery (2000 samples, 2 ms)

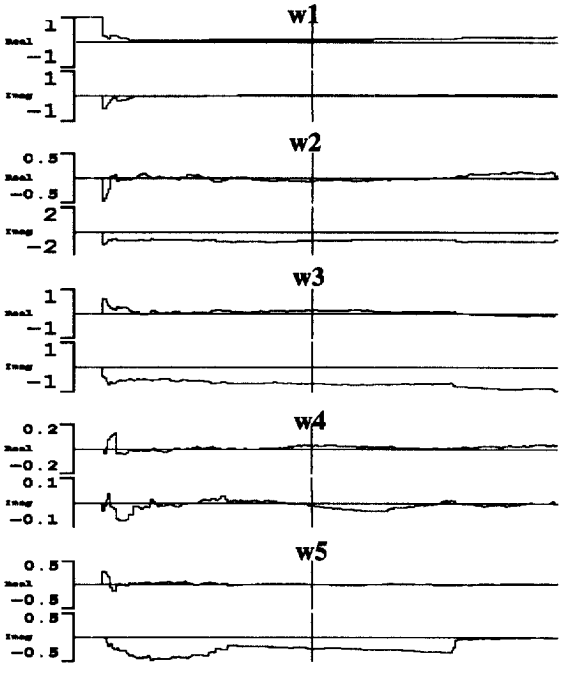

figure 9 : Weights during adaptation (2000 samples, 2 ms)

The MSE (figure 10) shows that the convergence can be obtained in 10 symbols.

The eye diagrams on sensor number one (SNR=12) and at the output shows qualitatively the improvement obtained by the combiner.

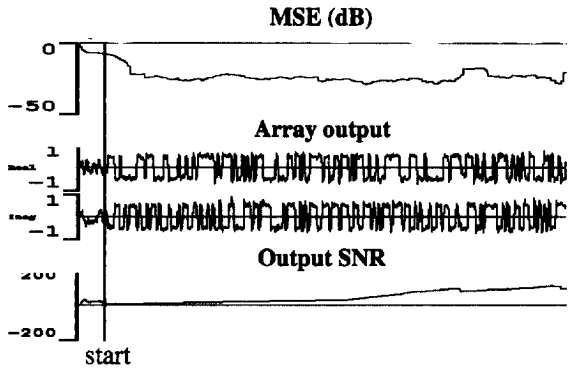

figure 10 : Algorithm results (2000 samples, 2 ms)

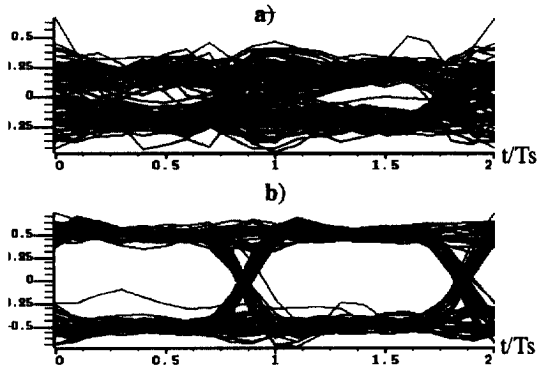

figure 11 : Eye diagram on sensor #1 (a) and at the array output (b) (1900 samples, 1.9 ms)

6.2. Statistical results

In this section statistical results are given for trials of the algorithm on 50 signals records. The SNR is estimated on each sensor and at the output of the array at the end of each record. Finally the output SNR is plotted versus the SNR averaged on each sensor.

Some remarks can be deduced from these results:

. A SNR improvement is obtained with the exception of for cases. But the difference is very small.

. The theoretical gain of five is rarely obtained

Table 1 gives the statistical results of the SNR obtained on the sensor #1, the mean obtained on the array and the output SNR.

. The mean SNR gain between the sensor #1 and the output and between the array and the output is respectively 3.27 and 2.36. The difference between these two values is due to the differences in the electronic of the receivers.

. The relative standard deviation is divided by two.

These two last values allow to quantify the improvement supplied by the combiner.

This improvement is not so important as a theoretical simplified analysis can predict. The difference can be attributed to some reasons:

- loss due to the demodulator and particularly to the carrier phase recovery which is not a simple task in the mobile-radio environment.

- loss in the case where one or some sensor signals is unworkable because the SNR is too small. This is the case when the mean level of the system is near the sensibility of the receiver.

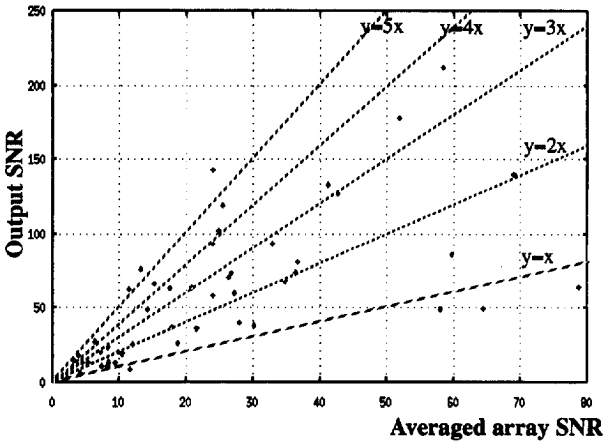

figure 12 : Output SNR versus averaged array SNR

Table 1 : Statistical results on the SNR

	sensor #1	Mean of the array	Output
Mean SNR	18	25	59
Standard deviation	4.7	4.4	6.8
Standard deviation (%)	26%	17%	11%

7. Conclusion

This paper has presented the experimental study of a multisensor receiver for mobile communications. A five sensors receiver was built in order to record the received signals in different situations. The measurements were carried out with different types of array in an urban area with sometimes cases of visibility.

The first process of the data shows that the SNR measured on the sensors after demodulation is uncorrelated.

An RLS algorithm was presented and implemented without the use of a reference signal.

Statistical results of the working of the algorithm show a mean gain of 2.36 on SNR.

8. Reference

[1] J. G.Proakis : « Digital Communications», McGraw-Hill, 1989.

Acknowledgment: This work was supported by CNET (convention 92 1B 179)